



Cone beam computed tomography-guided microwave ablation for hepatocellular carcinoma under the hepatic dome: a retrospective case-control study

Yiming Liu[^], Kunpeng Wu[^], Kaihao Xu[^], Chuan Tian[^], Dechao Jiao[^], Xinwei Han[^]

Department of Interventional Radiology, The First Affiliated Hospital of Zhengzhou University, Zhengzhou, China

Contributions: (I) Conception and design: Y Liu; (II) Administrative support: D Jiao, X Han; (III) Provision of study materials or patients: D Jiao, X Han; (IV) Collection and assembly of data: Y Liu, K Wu, C Tian; (V) Data analysis and interpretation: Y Liu, K Wu, K Xu; (VI) Manuscript writing: All authors; (VII) Final approval of manuscript: All authors.

Correspondence to: Dechao Jiao, PhD. Department of Interventional Radiology, The First Affiliated Hospital of Zhengzhou University, No. 1 Jianshe East Road, Zhengzhou, China. Email: jiaodechao007@126.com.

Background: Microwave ablation (MWA) for hepatocellular carcinoma (HCC) under the hepatic dome is still clinically challenging. This retrospective control study set out to analyze the technical application and clinical benefits of cone beam computed tomography (CBCT)-guided MWA for HCC under the hepatic dome.

Methods: The study analyzed 76 patients with 110 HCC lesions under the hepatic dome from April 2016 to January 2020. The patients were divided into two groups: (I) the CBCT group (n=31), in which iGuide navigation was used for the puncture, and (II) the conventional computed tomography (cCT) group (n=45), in which a navigation tool was not used for the puncture. The primary endpoints were technical success, puncture score, and the rates of complete ablation (CA), complications, and local tumor progression (LTP). The secondary endpoints were tumor-free survival (TFS) and overall survival (OS).

Results: In terms of the primary endpoints, the puncture score, occurrence of pleural effusion, and occurrence of right shoulder pain differed significantly between the CBCT group and the cCT group (2.8 *vs.* 2.2, $P=0.002$; 12.9% *vs.* 35.6%, $P=0.03$; 9.7% *vs.* 33.3%, $P=0.03$, respectively). However, the rates of technical success, CA, major complications, and LTP showed no significant differences between the two groups (100% *vs.* 100%, $P>0.009$; 0% *vs.* 0%, $P>0.009$; 95.6% *vs.* 89.2%, $P=0.30$; 4.5% *vs.* 4.6%, $P=0.96$, respectively). Regarding the secondary endpoints, the median TFS was 23.0 [95% confidence interval (CI): 19.5–26.5] *vs.* 22.0 (95% CI: 18.4–25.6) months ($P=0.41$) and the median OS was 31.0 (95% CI: 21.4–40.6) *vs.* 33.0 (95% CI: 27.9–38.2) months ($P=0.95$).

Conclusions: Cone beam CT is a feasible and effective image guidance tool for MWA of HCC under the hepatic dome.

Keywords: Cone beam computed tomography (CBCT); microwave ablation (MWA); hepatocellular carcinoma (HCC); clinical study

Submitted Feb 15, 2022. Accepted for publication Jul 13, 2022.

doi: 10.21037/qims-22-143

View this article at: <https://dx.doi.org/10.21037/qims-22-143>

[^] ORCID: Dechao Jiao, 0000-0002-5055-4672; Yiming Liu, 0000-0001-5898-9913; Kunpeng Wu, 0000-0001-6408-8927; Kaihao Xu, 0000-0002-3651-5773; Chuan Tian, 0000-0003-3311-5288; Xinwei Han, 0000-0003-4460-8619.

Introduction

According to a recent report, hepatocellular carcinoma (HCC) has the fourth highest incidence and the second highest mortality rate of all malignant tumors in China (1). With the advancement of minimally invasive interventional equipment and technology, local ablation techniques, such as microwave ablation (MWA) and radiofrequency ablation, have become the third-choice treatment for HCC following surgical resection and liver transplantation (2,3). The outcomes of ablation depend on three key factors—tumor visualization, applicator localization, and ablation evaluation—and optimal guidance tools must fulfill these requirements (4). Ultrasound (US) is the most popular guidance tool for HCC ablation. However, when the tumor is located under the hepatic dome, there is a limited sonic window, respiratory movement, and overlapping lung tissue (5,6); consequently, images obtained with US often appear blurred. Because of its high-density resolution, computed tomography (CT) is a good alternative guidance tool to US, but its puncture success rate depends heavily on the experience of the operator.

Cone beam CT (CBCT) differs from conventional CT (cCT) as it combines a digital flat-panel detector C-arm angiography system with improved CT reconstruction technology to generate CT-like multi-planar images with a spatial resolution of 1 mm and a density resolution of 5–10 HU (7). Moreover, the post-processing workstation has an iGuide virtual navigation system (VNS; Artis Zeego, Siemens, Germany), and the best puncture path can be planned on cross-sectional, coronal, and sagittal images. The navigation path integrates into the C-arm fluoroscopy image to guide the puncture in real time with the ablation applicator. Therefore, compared to cCT guidance, CBCT guidance may allow for shorter operative times and lower radiation doses. Further, CBCT can be used to assess lipiodol deposition in the lesion after transarterial chemoembolization (TACE), enabling easier identification and marking of the target lesion, especially for complex patients who receive multiple TACE treatments (8).

The above advantages make CBCT theoretically capable of being as reliable and efficient a guidance tool as cCT for puncture and ablation of HCC. Therefore, we conducted a controlled study using CBCT and cCT to explore the application and clinical benefits of CBCT-guided MWA for HCC under the hepatic dome. We present the following article in accordance with the STROBE reporting checklist (available at <https://qims.amegroups.com/article/>

[view/10.21037/qims-22-143/rc](https://doi.org/10.21037/qims-22-143/rc)).

Methods

Patients

From April 2016 to January 2020, 433 patients with HCC underwent MWA at the Department of Interventional Radiology in The First Affiliated Hospital of Zhengzhou University. A multidisciplinary oncology consultation group discussed all patients who underwent local ablation in our study. October 2018 [when our center introduced the multifunctional digital subtraction angiography (DSA) with DynaCT] was taken as a cut-off; before this date, MWA was done under cCT guidance, and after this date, MWA was done under CBCT guidance to explore its function.

The criteria for inclusion in the study were: (I) age 18–75 years; (II) a tumor located under the hepatic dome (distance between the intrahepatic tumor and the diaphragm, ≤ 5 mm) and not clearly detectable on US; (III) number of the liver lesions \leq and single tumor diameter ≤ 5 cm; (IV) Child-Pugh class A or B; (V) Eastern Cooperative Oncology Group (ECOG) score ≤ 2 ; (VI) platelet count $>40 \times 10^9/L$ and prothrombin time (PT) ≤ 25 s; and (VII) no portal vein thrombus or extrahepatic metastases. The exclusion criteria were: (I) a lack of evidence for HCC diagnosis based on the European Association for the Study of the Liver Criteria (9); (II) severe cardiopulmonary dysfunction; and (III) incomplete clinical data. The workflow is presented in *Figure 1*.

The study was conducted in accordance with the Declaration of Helsinki (as revised in 2013) and was approved by the Ethics Committee of The First Affiliated Hospital of Zhengzhou University. The requirement for individual consent for this retrospective analysis was waived.

Procedure

TACE

All patients underwent enhanced CT or magnetic resonance imaging (MRI) within 1 week before the operation. Thirty-one patients from the CBCT group and 41 from the cCT group underwent TACE before percutaneous MWA to localize the tumor and improve the MWA efficiency. Two interventional radiologists (XW Han and DC Jiao, with 25 and 15 years of experience, respectively) performed the procedures. All patients assumed a supine position before undergoing DSA (Artis Zeego, 30×40 cm flat detector,

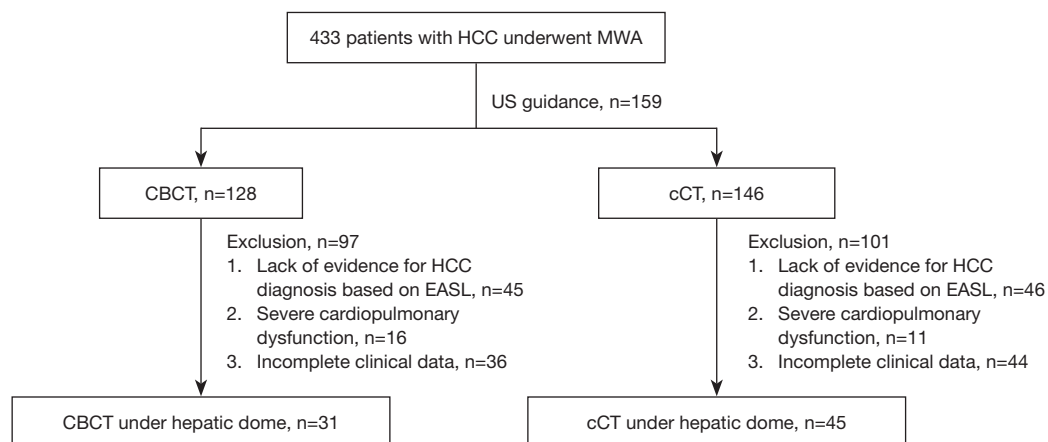


Figure 1 Workflow diagram of the study. HCC, hepatocellular carcinoma; MWA, microwave ablation; US, ultrasound; CBCT, cone beam computed tomography; cCT, conventional computed tomography; EASL, European Association for the Study of the Liver.

Siemens, Germany) with continuous electrocardiogram and blood pressure monitoring. Diloxin (5–10 mg) and dexmedetomidine (0.5 µg/kg) were injected intravenously 15–20 min before the procedure. A 2.7-F microcatheter (Terumo, Japan) was superselectively inserted into the tumor feeding artery. A mixture of 3.3–10.0 mL of lipiodol (Hengrui Medical, China) and 10–20 mg of doxorubicin (Main Luck Pharmaceuticals Inc., China) was used for embolization. Finally, polyvinyl alcohol (size 350–560 µm; Alikang Pharmaceutical Technology Co., Ltd., Hangzhou, China) was used to block the feeding artery. In cases of poor lipiodol uptake, the MWA was done as soon as possible because lipiodol deposition in normal liver tissue around the lesion can, for a short period, serve as a “marker” in combination with pre-treatment enhanced CT and MRI.

CBCT-guided percutaneous MWA

All punctures were performed by the two above-mentioned interventional radiologists. All CBCT images were obtained using flat-panel detector DSA (Artis Zeego, Siemens, Germany) with the patients holding their breaths for 8 seconds (C-arm rotation: 200°; X-ray dose: 0.36 µGy/frame; field of view: 480 mm). All raw data were transferred to Syngo X Workplace for volume reconstruction, and the CBCT images were displayed as cross-sectional, coronal, and sagittal images. To avoid damage to the lung and diaphragm, the puncture path was planned with iGuide VNS (a dedicated virtual puncture navigation software matched with Siemens’ CBCT). The procedure is demonstrated in *Figures 2–6*. The C-arm was adjusted to the bullseye view, with the C-arm distributed parallel to

the virtual puncture path. Using this view, the skin entry point and the puncture road are aligned. The skin entry and target tumor sites were positioned using a cross and a circle that were aligned. The navigation path was integrated into the live C-arm fluoroscopy image. Subsequently, after the induction of local anesthesia with 2% lidocaine (5 mL), the applicator with a 1.5-cm active tip (ECO-100E; frequency: 2,450 MHz; size: 2.0×165 mm; Medical Instrument Co., Ltd., Nanjing, China) was advanced into the lesion labeled with high-density lipiodol in the progression view. Finally, another CBCT image was acquired to localize the microwave applicator. The power (45–55 W) and time (5–8 min) for a single ablation circle were chosen according to the tumor size and the manufacturer’s recommendations.

cCT-guided percutaneous MWA

In the cCT group, the puncture was done without the use of a navigation tool. The same interventional radiologists mentioned above performed all the punctures. A 64-row CT scan was performed to localize the tumor in the axial CT image (Brilliance Big Bore, Siemens, Germany) with a current of 200 mA, a voltage of 120 kV, and a thickness of 3 mm. The basic principle of the puncture is to avoid damage to the diaphragm, lung tissue, and the ribs to the maximum possible extent. Based on the operator’s experience, all puncture routes would travel from the caudal to the cranial side, with the center of the tumor as the puncture target. Because the axial image showed no full view of the oblique puncture applicator, the puncture was performed using a step-by-step strategy until the microwave applicator reached the center of the tumor. The ablation

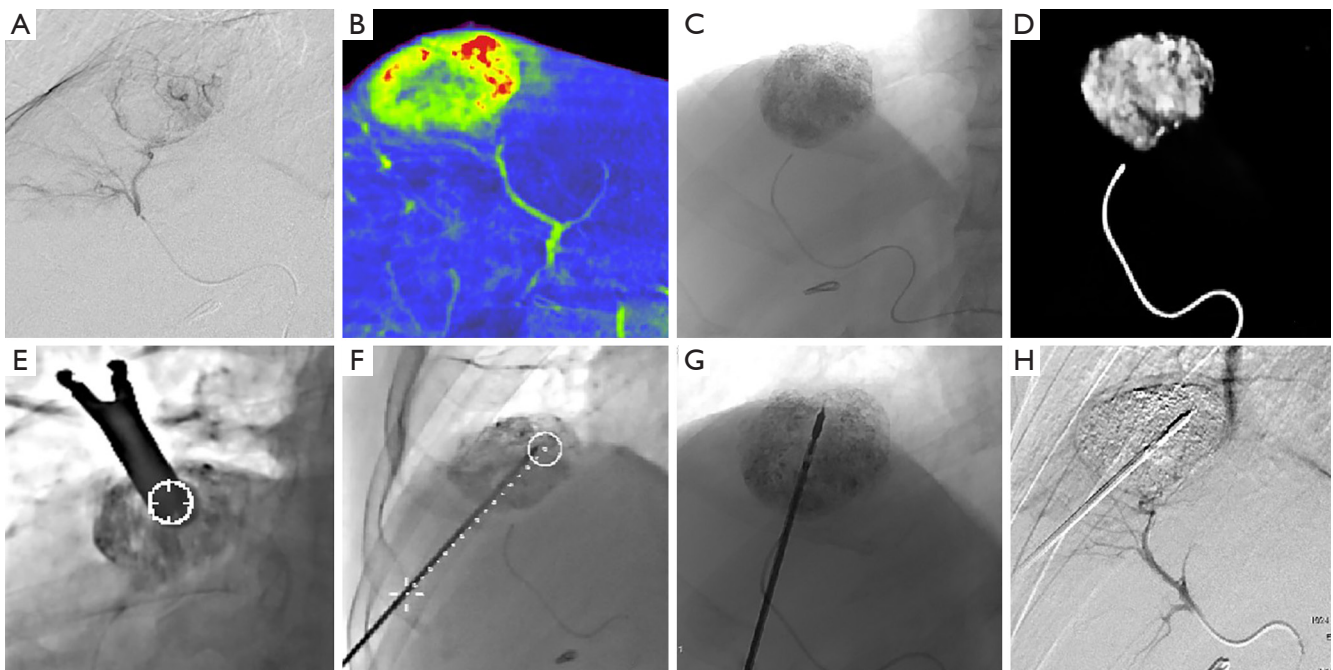


Figure 2 A 56-year-old man with a 4.8-cm HCC located under the hepatic dome. (A,B) Selective angiography of the anterior-superior subsegmental branch of the right hepatic artery showing a hypervascular tumor under the hepatic dome. (C,D) Embolization was performed, and the arterial blood supply was completely blocked on DSA or 3D images. (E,F) Real-time fluoroscopic images in bullseye view (E) and progression view (F). The needle was advanced along the planned needle path (white dotted line) from the skin entry site (white cross) to the target lesion site (white circle). (G,H) Images of TACE in combination with MWA. Tumor devascularization on angiography after MWA. HCC, hepatocellular carcinoma; DSA, digital subtraction angiography; 3D, three-dimensional; MWA, microwave ablation; TACE, transarterial chemoembolization.

parameters in the cCT group were the same as those described for the CBCT group.

Definitions and follow-up

The primary endpoints were the technical success rate, puncture score, the complete ablation (CA) rate, complications, and the local tumor progression (LTP) rate. The secondary endpoints included the tumor-free survival (TFS) and overall survival (OS). Technical success was defined as successful completion of the puncture and ablation. The punctures in the CBCT group and the cCT group, made using the iGuide VNS and without navigation, respectively, were assessed based on a score of 0–4 (Table 1). The ablation evaluation standards were the modified response evaluation criteria in solid tumors, or mRECIST, based on the image-guided tumor ablation: standardization of terminology and reporting criteria (10). CA was defined as uniform hypoattenuation (on CT or

MRI) without enhancement in the ablation area. Major complications were those that resulted in prolonged hospitalization or dysfunction, such as diaphragmatic perforation, hepatopulmonary abscess, massive hemorrhage, and fatal pneumothorax, and which had a Cardiovascular and Interventional Radiological Society of Europe (CIRSE) classification score of 4–6 (11). Minor complications were those with a CIRSE classification score of 1–3. LTP was defined as the ablation areas and adjacent areas that showed significant enhancement in the arterial phase and a fast-in and fast-out imaging pattern on enhanced CT or MRI during the follow-up period. TFS was defined as the time from the date of entry into the study to the first documented date of disease progression or death, or to the end of the study. OS was defined as the time from the date of entry into the study to the date of death or the last follow-up visit.

According to the follow-up plan, all patients underwent contrast-enhanced CT or MRI at 1-month intervals after

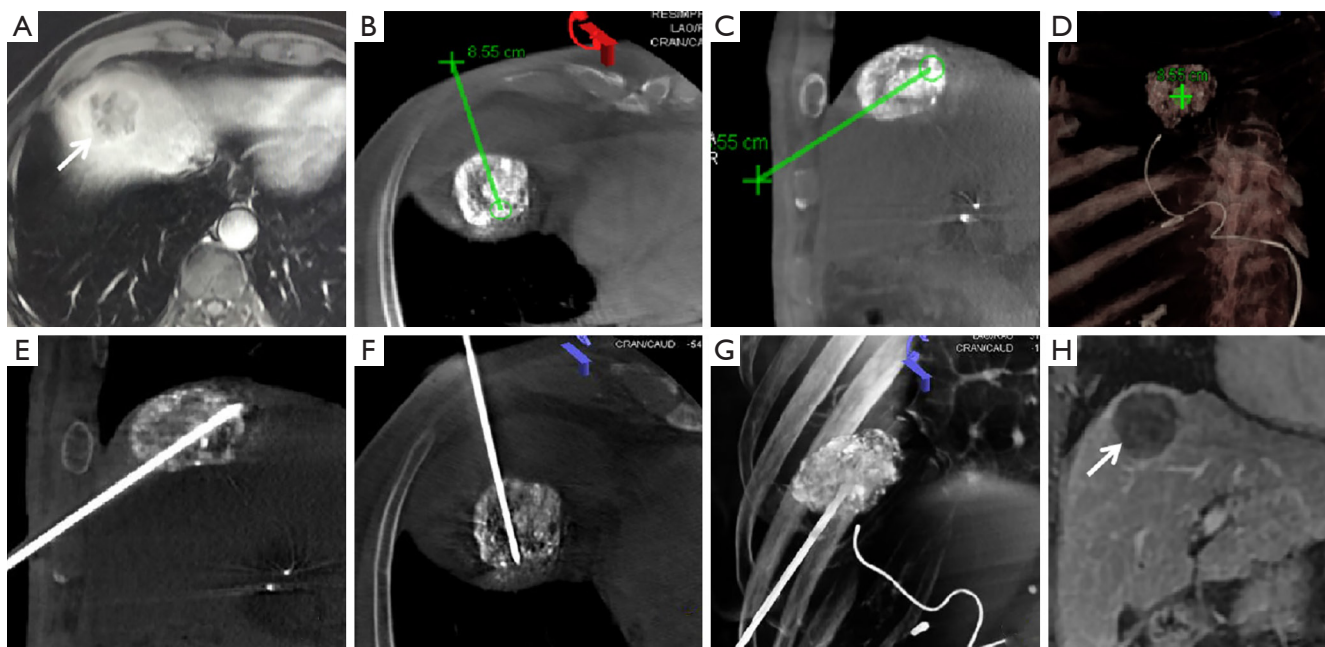


Figure 3 The same patient as shown in *Figure 2*. (A) Axial image of the contrast-enhanced CT before treatment showing the location of the tumor lesion (white arrow). (B-D) CBCT iGuide VNS multi-planar images with graphics showing the planned puncture path (green line) into the target lesion (green circle). (E-G) CBCT image confirming the position of the MWA applicator. (H) Coronal image showing CA of the tumor (white arrow) after 1 year. CT, computed tomography; CBCT, cone beam computed tomography; VNS, virtual navigation system; MWA, microwave ablation; CA, complete ablation.

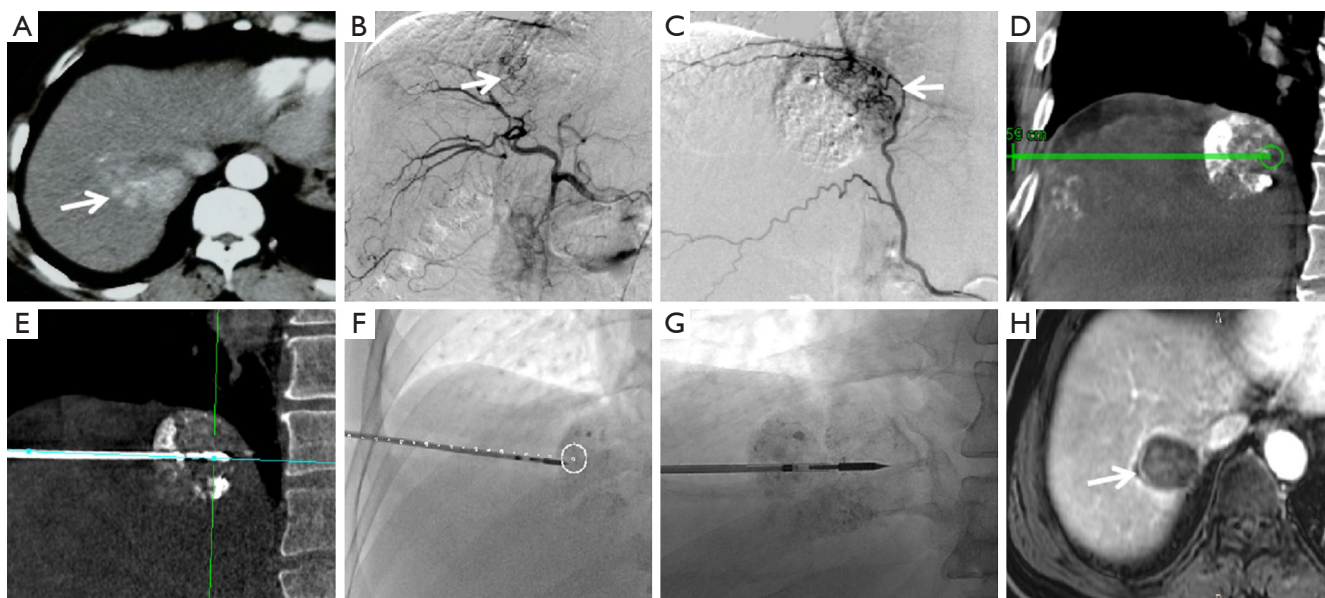


Figure 4 A 63-year-old man with a 4.6-cm HCC located under the hepatic dome. (A) Location of the tumor lesion (white arrow). (B,C) Selective angiography of the tumor feeding arteries was directed by the white arrow (phrenic artery and right hepatic artery). (D-G) CBCT iGuide VNS and real-time puncture under fluoroscopy. (H) Coronal image showing CA of the tumor after 6 months (white arrow). HCC, hepatocellular carcinoma; CBCT, cone beam computed tomography; VNS, virtual navigation system; CA, complete ablation.

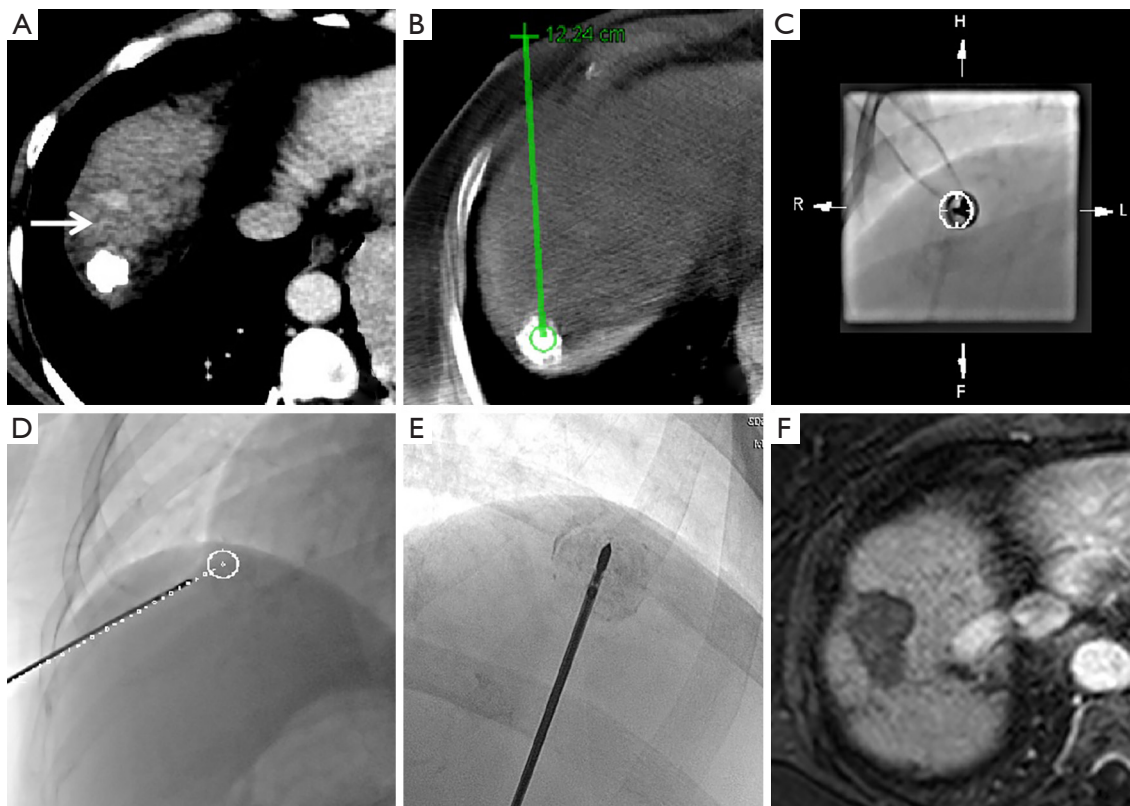


Figure 5 A 42-year-old woman with a 2.6-cm HCC with local progression after TACE. (A) Location of the tumor lesion (white arrow). (B) CBCT iGuide VNS and (C-E) real-time puncture under fluoroscopy. Axial-enhanced magnetic resonance image showing CA of the tumor after 6 months. HCC, hepatocellular carcinoma; TACE, transarterial chemoembolization; CBCT, cone beam CT; VNS, virtual navigation system; CA, complete ablation.

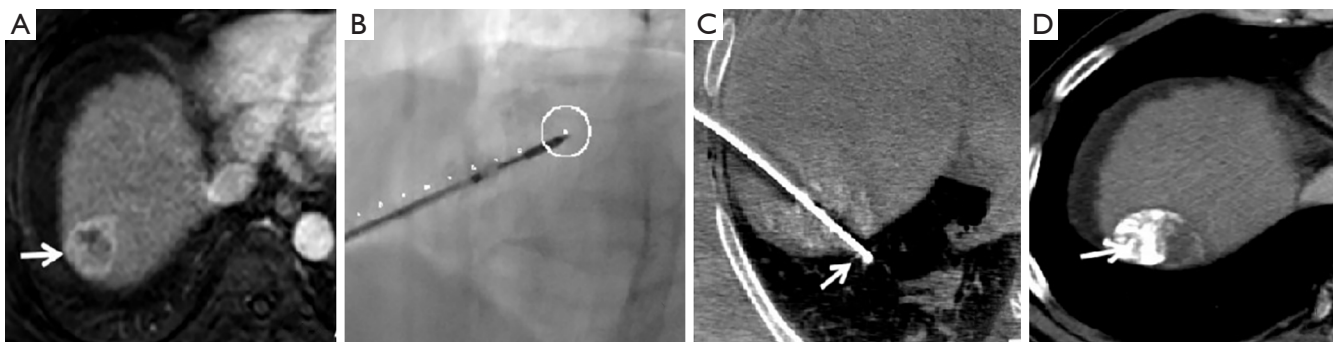


Figure 6 A 55-year-old woman with a 2.4-cm HCC located under the hepatic dome. (A) Location of the tumor lesion (white arrow). (B) iGuide VNS and real-time puncture under fluoroscopy. (C) Multi-planar immediate reconstruction image showing that the needle tip (white arrow) had entered the lung. The applicator had to be adjusted to avoid diaphragmatic perforation or lung injury; however, the position of the microwave applicator appeared normal on fluoroscopy. (D) Axial-enhanced CT image showing complete tumor ablation (white arrow) after 3 months. HCC, hepatocellular carcinoma; VNS, virtual navigation system; CT, computed tomography.

Table 1 Scoring standards for puncture performance

Score	Standards
0	Unsuccessful needle insertion
1	Successful puncture requiring >4 needle repositions for a single lesion
2	Successful puncture requiring 3–4 needle repositions for a single lesion
3	Successful puncture requiring 1–2 needle repositions for a single lesion
4	Successful first puncture

MWA. If the local lesion was evaluated as CA three times, the follow-up interval was changed to 3 months after MWA and every 3 months thereafter. All follow-up enhanced CT scans were evaluated based on consensus between two radiologists (DC Jiao and JZ Ren).

Statistical analyses

IBM SPSS (IBM, Armonk, USA) was used to perform all statistical analyses. Continuous variables were represented as the mean \pm standard deviation or the median. Baseline data were compared using the independent *t*-test, Pearson's χ^2 test, or Fisher's exact test. The independent *t*-test was used to compare the puncture score between the CBCT and cCT groups. The complications and local CA rates were analyzed using Pearson's χ^2 or Fisher's exact test. The Kaplan-Meier method was used to calculate TFS and OS. All tests were two-sided, and a P value of <0.05 was considered statistically significant.

Results

General data

All data were collected at The First Affiliated Hospital of Zhengzhou University. Of 433 HCC cases treated with ablation at the hospital, all except 159 cases underwent ablation under US guidance. The ablation was done under CBCT and cCT guidance in 128 and 146 cases, respectively; of these cases, 198 were excluded from this study (see *Figure 1*). Finally, 76 patients (including 65 cases of newly diagnosed HCC and 11 cases of HCC recurrence) with 110 lesions under the hepatic dome who underwent percutaneous MWA were included in the study. The patients were divided into two groups according to whether they underwent MWA under CBCT guidance using iGuide navigation for puncture (the CBCT group, n=31) or under cCT guidance without navigation for puncture (the cCT

group, n=45).

The mean maximum tumor diameters in the CBCT and cCT groups were (2.9 \pm 1.0) cm and (3.1 \pm 0.8) cm, respectively (P=0.39). The number of patients with 1, 2, and 3 lesions was 20, 8, and 3, respectively, in the CBCT group, and 29, 12, and 4, respectively, in the cCT group. No significant difference was observed in the number of lesions between the two groups (P=0.97). All patients had undergone TACE before receiving MWA. Twenty-three (74.2%) patients in the CBCT group underwent simultaneous TACE and MWA, and 41 (91.1%) patients in the cCT group underwent MWA at 3–14 days following TACE. Data including sex, age, liver cirrhosis, hepatitis, laboratory values, and the distance from the tumor to the hepatic dome are listed in *Table 2*; there were no significant differences between the two groups in these data (all P>0.05).

Primary endpoints

The technical success rate in both groups was 100%. The puncture score was higher in the CBCT group than in the cCT group [2.8 \pm 1.0 (range, 1–4) *vs.* 2.2 \pm 1.0 (range, 1–4), P=0.002]. In the CBCT group and the cCT group, there were 30 and 25 patients, respectively, with a puncture score of 3–4, and 15 and 40 patients, respectively, with a puncture score of 1–2. *Table 3* shows detailed information on the puncture score and the tumor location in the patients. Significant differences were observed in the number of patients with a puncture score of 3–4 between the two groups (P=0.007; *Table 4*). However, no significant differences were observed in the total procedure time [47.8 \pm 16.2 (range, 27–80) min in CBCT group *vs.* 50.1 \pm 13.8 (range, 33–79) min in cCT group, P=0.50]. No major complications occurred in either group.

During follow-up, there were significant differences between the CBCT and cCT groups in the occurrence of

Table 2 Baseline characteristics of all patients

Parameters	CBCT group (n=31)	cCT group (n=45)	P value
Sex			0.49
Male	17 (54.8)	26 (57.8)	
Female	14 (45.2)	19 (42.2)	
Mean age (years)	57.6±9.9	58.2±9.0	0.78
Liver cirrhosis			0.66
Child A	26 (83.9)	34 (75.6)	
Child B	3 (9.7)	7 (15.6)	
No cirrhosis	2 (6.4)	4 (8.8)	
Hepatitis			0.82
HBV	24 (77.4)	37 (90.2)	
HCV	5 (16.1)	5 (11.1)	
No hepatitis	2 (6.5)	3 (6.7)	
Laboratory data			
AFP (ng/mL)			0.57
≤200	14 (45.2)	20 (44.4)	
>200	17 (54.8)	25 (55.6)	
Total bilirubin (μmol/L)	16.8±6.1	15.9±6.2	0.55
Albumin (g/L)	41.3±4.6	40.7±5.0	0.59
Platelet (×10 ⁹ /L)	105.0±34.6	97.9±26.6	0.31
PT (s)	12.6±3.3	12.0±3.0	0.41
Creatinine (μmol/L)	66.9±18.1	65.9±13.1	0.78

Table 2 (continued)**Table 2** (continued)

Parameters	CBCT group (n=31)	cCT group (n=45)	P value
No. of lesions	45	65	0.97
1 lesion	20 (44.4)	29 (44.6)	
2 lesions	8 (35.6)	12 (36.9)	
3 lesions	3 (20.0)	4 (18.5)	
Tumor location	45	65	0.94
Segment VIII	21 (46.7)	28 (43.1)	
Segment VII	14 (31.1)	21 (32.3)	
Segment IV	8 (17.8)	14 (21.5)	
Segment II	2 (4.4)	2 (3.1)	
Max. diameter (cm)	2.9±1.0	3.1±0.8	0.39
Distance to hepatic dome (mm)	2.9±1.5	2.5±1.5	0.48
TACE assistance			0.15
Yes	31 (100.0)	41 (91.1)	
No	0 (0.0)	4 (8.9)	
ECOG score			0.96
0	18 (58.1)	26 (57.8)	
1	9 (29.0)	14 (31.1)	
2	4 (12.9)	5 (11.1)	

Data are presented as n (%) or mean ± SD. HBV, hepatitis B virus; HCV, hepatitis C virus; AFP, alpha fetoprotein; PT, prothrombin time; TACE, transarterial chemoembolization; ECOG, Eastern Cooperative Oncology Group; CBCT, cone beam computed tomography; cCT, conventional computed tomography.

Table 3 Detailed information on the puncture score and tumor locations

Parameters	CBCT group (n=31)				cCT group (n=45)				P value
	Score 4	Score 3	Score 2	Score 1	Score 4	Score 3	Score 2	Score 1	
S8	3	6	11	1	1	12	13	2	0.46
S7	3	10	1	0	1	7	10	3	0.01
S4	2	4	1	1	1	2	9	2	0.09
S2	1	1	0	0	0	1	1	0	0.37
Total	9	21	13	2	3	22	33	7	–

Data are presented as n. S, segment; CBCT, cone beam computed tomography; cCT, conventional computed tomography.

Table 4 Outcomes of HCC ablation under CBCT or cCT guidance

Parameters	CBCT group (n=31)	cCT group (n=45)	P value
Technical success for lesions	45/45 (100.0)	65/65 (100.0)	NA
Total procedure time	47.8±16.2	50.1±13.8	0.50
Puncture score	2.8±1.0	2.2±1.0	0.002
3–4	30	25	0.007
1–2	15	40	
Complications			
Major complications	0	0	NA
Minor complications			
Sub-capsular hematoma	3	4	0.90
Pneumothorax	0	5	0.08
Pleural effusion	4	16	0.03
Right shoulder pain	3	15	0.03
CA rate at 3 months	43/45	58/65	0.30
Local tumor progress	2/45	3/65	0.96

Data are presented as n/N (%), mean ± SD or n. HCC, hepatocellular carcinoma; CBCT, cone beam computed tomography; cCT, conventional computed tomography; CA, complete ablation; NA, not available.

right shoulder pain (9.7% vs. 33.3%, $P=0.03$) and pleural effusion (12.9% vs. 35.6%, $P=0.03$). In all cases, symptoms were alleviated within 1–3 weeks with conservative treatment. Pneumothorax (pulmonary compression of 5–20%, CIRSE grade 1) was observed in 5 patients in the cCT group during MWA. Although this complication did not occur among the patients in the CBCT group, there was no significant difference between the two groups (11% vs. 0%, $P=0.08$). Detailed information is presented in *Table 4*. At 3 months after ablation, the CA rate in the CBCT group and the cCT group was 95.5% (43/45) and 89.2% (58/65), respectively, and the LTP rate was 4.5% (2/45) and 4.6% (3/65), respectively. No significant differences were observed in the CA rate or the LTP rate between the two groups (all $P>0.05$).

Secondary endpoints

The 6-month, 1-year, and 2-year TFS rates were 93.5%, 87.1%, and 49.9%, respectively, in the CBCT group, and 93.3%, 79.8%, and 53.9%, respectively, in the cCT group. The median TFS was 23.0±1.8 [95% confidence interval (CI): 19.5–26.5] and 22.0±1.9 (95% CI: 18.4–25.6) months

in the CBCT and cCT groups, respectively. The log-rank test did not reveal any significant difference between the two groups ($P=0.41$).

During a median follow-up of 24 (range, 7–43) months, 29 patients (13 in the CBCT group and 16 patients in the cCT group) died. The 1-, 2-, and 3-year OS rates were 93.5%, 75.5%, and 41.4%, respectively, in the CBCT group, and 93.2%, 71.4%, and 45.7%, respectively, in the cCT group. The median OS was 31.0±4.9 (95% CI: 21.4–40.6) and 33.0±2.6 (95% CI: 27.9–38.2) months in the CBCT and cCT groups, respectively. The log-rank test did not reveal any significant difference between the two groups ($P=0.95$; *Figure 7*).

Discussion

With the development of instruments and therapeutic schemes, MWA is increasingly used in many medical institutions worldwide to treat small and large HCCs and other solid tumors (12–14). In China, US is the most common image guidance tool for ablation, followed by CT. Although US provides real-time images that are inexpensive, rapid, and easy to obtain, gas formation in the ablation

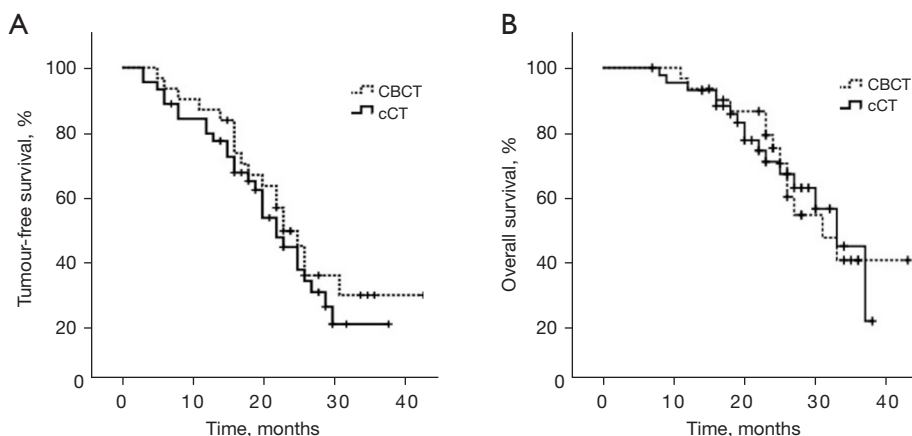


Figure 7 Comparison of TFS and OS in the CBCT and cCT groups. (A) The curve of TFS. (B) The curve of OS. CBCT, cone beam computed tomography; cCT, conventional computed tomography; TFS, tumor-free survival; OS, overall survival.

region and the patient's physical condition pose challenges for its use in identifying a safe path for tumor puncture, especially for lesions located under the hepatic dome (15). Some surgeons have attempted artificial hydrothorax (16), artificial ascites (17), laparoscopic assistance (18), and CT-fluoroscopy (19) to avoid injury to the diaphragm and prevent pneumothorax, all of which have been proven as useful methods. Although a previous study reported the possibility of a cCT-guided transthoracic puncture, the risk of pneumothorax with this technique was greatly increased and 18% of patients require closed chest drainage (20). cCT provides a more direct cross-sectional puncture path but lacks direct viewing dynamic guidance. Therefore, it is essential to find another tool to help perform cranio-caudal puncture, especially for inexperienced operators.

CBCT uses flat detector technology to achieve better spatial resolution, and the signal-to-noise ratio is lower than that of cCT due to higher scattering. It can obtain a rich volume of CT information and real-time fluoroscopy functions, and the system has its own iGuide VNS. Relative to cCT guidance, CBCT guidance allows for higher lesion localization accuracy, a shorter operative time, and flexibility—the direction and angle of the needle can be detected and adjusted in real-time depending on the location of the lesions. Moreover, CBCT facilitates simultaneous TACE and MWA without needing to transfer patients to the CT room for ablation, which can shorten the procedure time and reduce the risk to the patient. Further, unlike the microbubbles produced by ablation and the lipiodol deposited after TACE, which are limiting factors for the localization of target lesions by US, the

lipiodol deposited within the lesion after TACE allows for easier identification of the target lesion under CBCT. Some studies have shown that CBCT might be the best navigation tool for an oblique puncture (21,22). However, CBCT has some technical disadvantages, such as low resolution, irradiation exposure, cumbersome procedures, an unclear ablation boundary, and the strict requirement for breath-holding during image acquisition.

In the present study, a puncture score of 3–4 was observed in 66.7% and 40% of patients in the CBCT and cCT groups, respectively. Stratified analysis showed that the iGuide VNS was a useful tool for difficult punctures—such as tumors located at S7, which required non-coplanar puncture and a high puncture skill level—and may help to overcome the disadvantage of high dependency on the operator's experience when using cCT guidance. Moreover, the real-time dynamic guided puncture path is more intuitive and clearer under fluoroscopy, and requires less puncture readjustment, which allows for some relative reduction in the exposure time and radiation dose.

We searched PubMed with the keywords “microwave ablation”, “liver tumor”, and “close to diaphragm”. Eight papers published over the last decade reported technical success in 93–100% of cases, a complications rate of 0–23.6%, and an LTP rate of 0–18.8% (23–30) (Table 5). The technical success rate, major complications rate, and LTP rate in the present study were 100%, 0%, and 4.5%, respectively, all of which fall within the ranges in the literature. The CA rate, LTP rate, TFS, and OS were not significantly different between the two groups. This result is not surprising because, although the guidance tool was

Table 5 Results of recent clinical studies on MWA of liver tumors under the hepatic dome

Author	Design/sample	Tumor	LTP	Major complications	Long-term status
Hermida (23)	RS/56	HCC	10.7% LTP in CT with APE	No	MWA with APE is efficacious
Gao (24)	RS/103	HCC + LM	11.6%/15.0% LTP in study/ control group	No	TFS was 23.7/22.1 months in study/control group
Asvadi (25)	RS/46	HCC + LM	CA was 94.0%	Severe PN (4.4%)	OS was 73.9% over 24.9 months
Smolock (26)	RS/42	HCC + LM	5.5% LTP	No	NA
Wang (27)	RS/11	HCC	1 (7.1%) case had LTP	No	NA
Zhang (28)	RS/102	HCC + LM	1-, 2-, 3-year LTP in APE group were 13.4%, 17.1% and 17.1%	No	1-, 2-, 3-year TFS in APE group was 65.8%, 53.6%, and 53.6%
Li (29)	RS/89	HCC + LM	18.8% (18/96) LTP	No	NA
Liu (30)	RS/20	HCC + LM	CA rate was 84.2% (16/19)	Severe PN (5.0%)	NA

MWA, microwave ablation; RS, retrospective study; HCC, hepatocellular carcinoma; LM, liver metastases; LTP, local tumor progression; CT, computed tomography; APE, artificial pleural effusion; CA, complete ablation; PN, pneumothorax; TFS, tumor-free survival; OS, overall survival; NA, not available.

different, the subsequent ablation and follow-up strategy were the same for both groups. Further, in the 5 patients in the study who experienced local progression, 2 lesions (segment VII) were located close to the inferior vena cava and 3 were close to the hepatic vein (segment VIII), which may be related to the “heat sink effect” of local blood flow. It is worth mentioning that, in theory, when small lesions under the hepatic dome are locally ablated, the breathing amplitude of the patient and movement of the liver will increase due to local discomfort, which may result in applicator displacement. However, the tip of the applicator can be monitored during MWA by fluoroscopy, which can prevent displacement (31).

All patients underwent TACE before undergoing MWA, and 74.2% (23/31) of the patients in the CBCT group underwent the two procedures simultaneously. Combined treatment with TACE and thermal ablation is not generally recommended for intrahepatic tumor sizes ≤ 3 cm because ablation monotherapy is equally as effective.

However, patients with tumors located under the hepatic dome have demonstrated high LTP rates of up to 29% at the 1-year follow-up (32). Yamakado *et al.* (33) and Hyun *et al.* (34) reported that combined therapy could decrease the long-term LTP rate. Takuma *et al.* (35) and Kagawa *et al.* (36) reported obvious advantages of combination strategies. For example, they found that performing TACE before MWA could reduce or block the blood supply to the local tumor, thereby improving the ablation efficiency. They also found that DSA can detect and embolize small lesions

that are not identified on pre-treatment images, and that high-density lipiodol acts as a marker that enables clearer visualization of the tumor boundary on a CBCT scan.

Assessment of the coagulation necrosis area is the most important index to evaluate the efficiency of ablation and reduce LTP. Several previous clinical studies have confirmed that the main factors for LTP are the existence of satellite HCCs and an insufficient safety margin during ablation (37,38). Satellite HCCs can be identified using DSA, while the ablation margin mainly depends on the image evidence obtained following ablation. According to the 2019 Chinese clinical guidelines for the management of HCC, the basic requirement for ablation is that the margin should be at least 5 mm beyond the boundary of the tumor at the three-dimensional (3D) level (39). Both CT, especially enhanced CT, and US can be used to judge the ablation area during and after the operation depending on the change of density or echo, which is widely accepted by ablation experts. This finding was not decided on in an animal study; rather, it was made according to the previous long-term clinical follow-up image data and the concept of surgical resection. Wang *et al.* (40) and Kurilova *et al.* (41) reported that an ablation margin of 5 mm beyond the primary tumor could significantly reduce LTP. Some scholars have developed dedicated 3D software and 3D quantitative assessment tools based on enhanced CT image fusion to objectively evaluate the safety margin (42-44). Density changes and bubbles occurring on the CT image may help the operator to roughly judge whether the tumor is completely ablated.

The extent of tumor ablation may not be clear on CBCT due to its poor density resolution. The low density of the ablation boundary needs to be adjusted to a certain window width to display it on CBCT, which may be considered the chief shortcoming of CBCT-guided ablation. For comprehensive evaluation of the ablation range, the following assessment parameters have been adopted at our center: (I) visualization of the low-density area after ablation at a window width of 100–300 HU and window level of 30–40 HU; (II) disappearance of tumor vessels on post-ablation angiography or enhanced CT, indicating CA; and (III) personal experience of the MWA procedure. CBCT can simultaneously combine angiography and CT-like multi-planar images. Further, hepatic perfusion imaging might be a good tool to evaluate the range of ablation, which will be the focus of our next research project.

Pleural effusion and right shoulder pain might be attributable to the following: (I) tumor location, especially tumors located at S8 and S7, of which there were 49 and 35 cases in the cCT and CBCT groups, respectively; (II) tumor size, which was larger in the cCT group (3.1 cm) than the CBCT group (2.9 cm), although it showed no statistically significant difference. Pain was also considered to be a symptom triggered by the transfer of thermal energy to the adjacent diaphragm and causing mild damage to the diaphragm (23); (III) large right lower lung movement and damage due to puncture adjustment. A lack of real-time guidance in the cCT group resulted in more frequent puncture adjustment and more damage than in the CBCT group. These symptoms were less common in the CBCT group than in the cCT group, which indicates that there was less heat-related damage to the diaphragm with the former approach. It is believed that three factors contribute to the diaphragm's thermal injury: puncture path/depth, MWA power, and ablation time. Most tumors located under the hepatic dome can be completely ablated without artificial ascites or hydrodissection by selecting the appropriate path of the puncture.

Further, in addition to our strategy of low power (45–55 W) and a short ablation time (5–8 min) for a single ablation circle, the iGuide VNS and multi-planar immediate reconstruction ensured a more accurate puncture. For example, in one female patient, the position of the microwave applicator was normal on fluoroscopy (Figure 6), but the immediate reconstructed image showed that the needle tip had entered the lung, which indicated that the applicator needed to be adjusted to avoid diaphragmatic perforation or lung injury.

This study has certain limitations, such as the small sample size and inclusion of only small tumors (with a mean diameter of <3 cm). Also, the median follow-up time was 24 months, which is short. Considering the retrospective design of the study, the statistical power is also low. Finally, the iGuide VNS is simple to use but poses a learning curve for beginners. Future multicenter prospective studies with a large sample size will be needed to validate the findings presented in this research.

In conclusion, our study results suggest that CBCT guidance is a feasible and effective imaging guidance tool for MWA of HCC under the hepatic dome.

Acknowledgments

Funding: This work was supported by the Provincial and Ministerial Youth Project and the Henan Medical Science and Technology Public Relations Program (No. SB201902014).

Footnote

Reporting Checklist: The authors have completed the STROBE reporting checklist. Available at <https://qims.amegroups.com/article/view/10.21037/qims-22-143/rc>

Conflicts of Interest: All authors have completed the ICMJE uniform disclosure form (available at <https://qims.amegroups.com/article/view/10.21037/qims-22-143/coif>). The authors have no conflicts of interest to declare.

Ethical Statement: The authors are accountable for all aspects of the work in ensuring that questions related to the accuracy or integrity of any part of the work are appropriately investigated and resolved. The study was conducted in accordance with the Declaration of Helsinki (as revised in 2013). The study was approved by the Ethics Committee of The First Affiliated Hospital of Zhengzhou University, and individual consent for this retrospective analysis was waived.

Open Access Statement: This is an Open Access article distributed in accordance with the Creative Commons Attribution-NonCommercial-NoDerivs 4.0 International License (CC BY-NC-ND 4.0), which permits the non-commercial replication and distribution of the article with the strict proviso that no changes or edits are made and the original work is properly cited (including links to both the

formal publication through the relevant DOI and the license).
See: <https://creativecommons.org/licenses/by-nc-nd/4.0/>.

References

- Zhu F, Rhim H. Thermal ablation for hepatocellular carcinoma: what's new in 2019. *Chin Clin Oncol* 2019;8:58.
- Chen J, Lin Z, Lin Q, Lin R, Yan Y, Chen J. Percutaneous radiofrequency ablation for small hepatocellular carcinoma in hepatic dome under MR-guidance: clinical safety and efficacy. *Int J Hyperthermia* 2020;37:192-201.
- Wang M, Xu F, Yu Y, Xing L, Gu C, Meng D. Treatment of a special-located occult hepatic cancer in a cirrhotic patient using laparoscopic ultrasound-guided radiofrequency ablation: a case description. *Quant Imaging Med Surg* 2021;11:4475-8.
- Xu EJ, Lv SM, Li K, Long YL, Zeng QJ, Su ZZ, Zheng RQ. Immediate evaluation and guidance of liver cancer thermal ablation by three-dimensional ultrasound/contrast-enhanced ultrasound fusion imaging. *Int J Hyperthermia* 2018;34:870-6.
- Marinetto E, Uneri A, De Silva T, Reangamornrat S, Zbijewski W, Sisniega A, Vogt S, Kleinszig G, Pascau J, Siewerdsen JH. Integration of free-hand 3D ultrasound and mobile C-arm cone-beam CT: Feasibility and characterization for real-time guidance of needle insertion. *Comput Med Imaging Graph* 2017;58:13-22.
- Jiao DC, Han XW, Wu G, Ren JZ. 3D CACT-assisted Radiofrequency Ablation Following Transarterial Chemoembolization for Hepatocellular Carcinoma: Early Experience. *Asian Pac J Cancer Prev* 2015;16:7897-903.
- Liu J, Yan H, Cheng H, Liu J, Sun P, Wang B, Mao R, Du C, Luo S. CBCT-based synthetic CT generation using generative adversarial networks with disentangled representation. *Quant Imaging Med Surg* 2021;11:4820-34.
- Heerink WJ, Ruiters SJS, Pennings JP, Lansdorp B, Vliegenthart R, Oudkerk M, de Jong KP. Robotic versus Freehand Needle Positioning in CT-guided Ablation of Liver Tumors: A Randomized Controlled Trial. *Radiology* 2019;290:826-32.
- Ayuso C, Rimola J, Vilana R, Burrel M, Darnell A, García-Criado Á, Bianchi L, Belmonte E, Caparroz C, Barrufet M, Bruix J, Brú C. Diagnosis and staging of hepatocellular carcinoma (HCC): current guidelines. *Eur J Radiol* 2018;101:72-81.
- Ahmed M, Solbiati L, Brace CL, Breen DJ, Callstrom MR, Charboneau JW, et al. Image-guided tumor ablation: standardization of terminology and reporting criteria--a 10-year update. *Radiology* 2014;273:241-60.
- Filippiadis DK, Binkert C, Pellerin O, Hoffmann RT, Krajina A, Pereira PL. Cirse Quality Assurance Document and Standards for Classification of Complications: The Cirse Classification System. *Cardiovasc Intervent Radiol* 2017;40:1141-6.
- Xie L, Cao F, Qi H, Song Z, Shen L, Chen S, Hu Y, Chen C, Fan W. Efficacy and safety of CT-guided percutaneous thermal ablation for hepatocellular carcinoma adjacent to the second porta hepatis. *Int J Hyperthermia* 2019;36:1122-8.
- Wang D, Li B, Bie Z, Li Y, Li X. Synchronous core-needle biopsy and microwave ablation for highly suspicious malignant pulmonary nodule via a coaxial cannula. *J Cancer Res Ther* 2019;15:1484-9.
- Cui R, Wang XH, Ma C, Liu T, Cheng ZG, Han ZY, Liu FY, Yu XL, Yu J, Liang P. Comparison of Microwave Ablation and Transarterial Chemoembolization for Single-Nodule Hepatocellular Carcinoma Smaller Than 5cm: A Propensity Score Matching Analysis. *Cancer Manag Res* 2019;11:10695-704.
- An C, Cheng Z, Yu X, Han Z, Liu F, Li X, Wu SS, Yu J, Liang P. Ultrasound-guided percutaneous microwave ablation of hepatocellular carcinoma in challenging locations: oncologic outcomes and advanced assistive technology. *Int J Hyperthermia* 2020;37:89-100.
- Long Y, Zeng Q, He X, Ye H, Su Y, Zheng R, Yu J, Xu E, Li K. One-lung ventilation for percutaneous thermal ablation of liver tumors in the hepatic dome. *Int J Hyperthermia* 2020;37:49-54.
- Hsieh YC, Limquiaco JL, Lin CC, Chen WT, Lin SM. Radiofrequency ablation following artificial ascites and pleural effusion creation may improve outcomes for hepatocellular carcinoma in high-risk locations. *Abdom Radiol (NY)* 2019;44:1141-51.
- Chen L, Zhang L, Tian M, Hu Q, Zhao L, Xiong J. Safety and effective of laparoscopic microwave ablation for giant hepatic hemangioma: A retrospective cohort study. *Ann Med Surg (Lond)* 2019;39:29-35.
- Mitani H, Naito A, Chosa K, Kodama H, Sumida M, Moriya T, Awai K. Safety margin for CT- and US-guided radiofrequency ablation after TACE of HCC in the hepatic dome. *Minim Invasive Ther Allied Technol* 2022;31:894-901.
- Cazzato RL, Buy X, Alberti N, Fonck M, Grasso RF, Palussière J. Flat-panel cone-beam CT-guided radiofrequency ablation of very small (≤ 1.5 cm) liver

- tumors: technical note on a preliminary experience. *Cardiovasc Intervent Radiol* 2015;38:206-12.
21. Jiao D, Xie N, Wu G, Ren J, Han X. C-arm cone-beam computed tomography with stereotactic needle guidance for percutaneous adrenal biopsy: initial experience. *Acta Radiol* 2017;58:617-24.
 22. Jiao D, Yuan H, Zhang Q, Han X. Flat detector C-arm CT-guided transthoracic needle biopsy of small (≤ 2.0 cm) pulmonary nodules: diagnostic accuracy and complication in 100 patients. *Radiol Med* 2016;121:268-78.
 23. Hermida M, Cassinotto C, Piron L, Assenat E, Pageaux GP, Escal L, Pierredon-Foulongne MA, Verzilli D, Jaber S, Guiu B. Percutaneous thermal ablation of hepatocellular carcinomas located in the hepatic dome using artificial carbon dioxide pneumothorax: retrospective evaluation of safety and efficacy. *Int J Hyperthermia* 2018;35:90-6.
 24. Gao F, Wang GB, Xiang ZW, Yang B, Xue JB, Mo ZQ, Zhong ZH, Zhang T, Zhang FJ, Fan WJ. A preoperative mathematic model for computed tomographic guided microwave ablation treatment of hepatic dome tumors. *Oncotarget* 2016;7:25949-59.
 25. Asvadi NH, Anvari A, Uppot RN, Thabet A, Zhu AX, Arellano RS. CT-Guided Percutaneous Microwave Ablation of Tumors in the Hepatic Dome: Assessment of Efficacy and Safety. *J Vasc Interv Radiol* 2016;27:496-502; quiz 503.
 26. Smolock AR, Lubner MG, Ziemelewick TJ, Hinshaw JL, Kitchin DR, Brace CL, Lee FT Jr. Microwave ablation of hepatic tumors abutting the diaphragm is safe and effective. *AJR Am J Roentgenol* 2015;204:197-203.
 27. Wang G, Sun Y, Cong L, Jing X, Yu J. Artificial pleural effusion in percutaneous microwave ablation of hepatic tumors near the diaphragm under the guidance of ultrasound. *Int J Clin Exp Med* 2015;8:16765-71.
 28. Zhang D, Liang P, Yu X, Cheng Z, Han Z, Yu J, Liu F. The value of artificial pleural effusion for percutaneous microwave ablation of liver tumour in the hepatic dome: a retrospective case-control study. *Int J Hyperthermia* 2013;29:663-70.
 29. Li M, Yu XL, Liang P, Liu F, Dong B, Zhou P. Percutaneous microwave ablation for liver cancer adjacent to the diaphragm. *Int J Hyperthermia* 2012;28:218-26.
 30. Liu LN, Xu HX, Lu MD, Xie XY. Percutaneous ultrasound-guided thermal ablation for liver tumor with artificial pleural effusion or ascites. *Chin J Cancer* 2010;29:830-5.
 31. Yuan H, Liu F, Li X, Guan Y, Wang M. Transcatheter arterial chemoembolization combined with simultaneous DynaCT-guided radiofrequency ablation in the treatment of solitary large hepatocellular carcinoma. *Radiol Med* 2019;124:1-7.
 32. Kang TW, Rhim H, Kim EY, Kim YS, Choi D, Lee WJ, Lim HK. Percutaneous radiofrequency ablation for the hepatocellular carcinoma abutting the diaphragm: assessment of safety and therapeutic efficacy. *Korean J Radiol* 2009;10:34-42.
 33. Yamakado K, Nakatsuka A, Takaki H, Sakurai H, Isaji S, Yamamoto N, Shiraki K, Takeda K. Subphrenic versus nonsubphrenic hepatocellular carcinoma: combined therapy with chemoembolization and radiofrequency ablation. *AJR Am J Roentgenol* 2010;194:530-5.
 34. Hyun D, Cho SK, Shin SW, Park KB, Lee SY, Park HS, Choo SW, Do YS. Combined transarterial chemoembolization of the right inferior phrenic artery and radiofrequency ablation for small hepatocellular carcinoma near the diaphragm: its efficacy and safety. *Abdom Radiol (NY)* 2018;43:2851-8.
 35. Takuma Y, Takabatake H, Morimoto Y, Toshikuni N, Kayahara T, Makino Y, Yamamoto H. Comparison of combined transcatheter arterial chemoembolization and radiofrequency ablation with surgical resection by using propensity score matching in patients with hepatocellular carcinoma within Milan criteria. *Radiology* 2013;269:927-37.
 36. Kagawa T, Koizumi J, Kojima S, Nagata N, Numata M, Watanabe N, Watanabe T, Mine T; Tokai RFA Study Group. Transcatheter arterial chemoembolization plus radiofrequency ablation therapy for early stage hepatocellular carcinoma: comparison with surgical resection. *Cancer* 2010;116:3638-44.
 37. Fukuda K, Mori K, Hasegawa N, Nasu K, Ishige K, Okamoto Y, Shiigai M, Abei M, Minami M, Hyodo I. Safety margin of radiofrequency ablation for hepatocellular carcinoma: a prospective study using magnetic resonance imaging with superparamagnetic iron oxide. *Jpn J Radiol* 2019;37:555-63.
 38. Lee MW, Kang D, Lim HK, Cho J, Sinn DH, Kang TW, Song KD, Rhim H, Cha DI, Lu DSK. Updated 10-year outcomes of percutaneous radiofrequency ablation as first-line therapy for single hepatocellular carcinoma < 3 cm: emphasis on association of local tumor progression and overall survival. *Eur Radiol* 2020;30:2391-400.
 39. Xie DY, Ren ZG, Zhou J, Fan J, Gao Q. 2019 Chinese clinical guidelines for the management of hepatocellular carcinoma: updates and insights. *Hepatobiliary Surg Nutr* 2020;9:452-63.

40. Wang X, Sofocleous CT, Erinjeri JP, Petre EN, Gonen M, Do KG, Brown KT, Covey AM, Brody LA, Alago W, Thornton RH, Kemeny NE, Solomon SB. Margin size is an independent predictor of local tumor progression after ablation of colon cancer liver metastases. *Cardiovasc Intervent Radiol* 2013;36:166-75.
41. Kurilova I, Gonzalez-Aguirre A, Beets-Tan RG, Erinjeri J, Petre EN, Gonen M, Bains M, Kemeny NE, Solomon SB, Sofocleous CT. Microwave Ablation in the Management of Colorectal Cancer Pulmonary Metastases. *Cardiovasc Intervent Radiol* 2018;41:1530-44.
42. Solbiati M, Muglia R, Goldberg SN, Ierace T, Rotilio A, Passera KM, Marre I, Solbiati L. A novel software platform for volumetric assessment of ablation completeness. *Int J Hyperthermia* 2019;36:337-43.
43. Li Z, Jiao D, Han X, Si G, Li Y, Liu J, Xu Y, Zheng B, Zhang X. Transcatheter arterial chemoembolization combined with simultaneous DynaCT-guided microwave ablation in the treatment of small hepatocellular carcinoma. *Cancer Imaging* 2020;20:13.
44. Kim YS, Lee WJ, Rhim H, Lim HK, Choi D, Lee JY. The minimal ablative margin of radiofrequency ablation of hepatocellular carcinoma (> 2 and < 5 cm) needed to prevent local tumor progression: 3D quantitative assessment using CT image fusion. *AJR Am J Roentgenol* 2010;195:758-65.

Cite this article as: Liu Y, Wu K, Xu K, Tian C, Jiao D, Han X. Cone beam computed tomography-guided microwave ablation for hepatocellular carcinoma under the hepatic dome: a retrospective case-control study. *Quant Imaging Med Surg* 2022;12(10):4837-4851. doi: 10.21037/qims-22-143